TITLE PAGE

Citation Format:

V. Damagatla, L. Di Sieno, A. Farina, A. Dalla Mora, and A. Pifferi, "Broadband non-contact spectroscopy using time-domain diffuse optics," in Diffuse Optical Spectroscopy and Imaging X, D. Contini, Y. Hoshi, and T. D. O'Sullivan, eds., Proc. of SPIE-Optica Vol. 13935, 1393513 (2025); https://doi.org/10.1117/12.3098386

DOI abstract link:

https://doi.org/10.1117/12.3098386

Broadband non-contact spectroscopy using time-domain diffuse optics

Vamshi Damagatla,[1,*] Laura Di Sieno,[1,2] Andrea Farina,[1] Alberto Dalla Mora,[1] Antonio Pifferi,[1,2]

[1] *Politecnico di Milano, Dipartimento di Fisica, Milan, 20133, Italy*
[2] *Istituto di Fotonica e Nanotecnologie, Consiglio Nazionale delle Ricerche, 20133, Milan, Italy*

[*] *saivamshi.damagatla@polimi.it*

Abstract: We perform non-contact broadband spectroscopy at a height of 7cm using time-domain diffuse optical techniques by utilizing a superconducting nanowire detector. We measure phantoms of water and lipids and also performed a preliminary in-vivo study.

1. Introduction

Time-domain diffuse optical spectroscopy(TD-DOS) – based on the detection of the distribution of time-of-flight (DTOF) of photons traveling into the tissue – has been a fast growing optical technique to non-invasively obtain information from human body which acts as a diffusive medium [1]. The combination of non-contact spectroscopy (NCS) with TD-DOS presents many advantages. Firstly, by removing probe contact, it limits contact-based artefacts from measurements. Further, it could be of extreme usefulness in applications where contact can be harmful, such as burn victims, skin-affliction patients, monitoring during surgery, to name a few. It also represents a shift towards a monitoring-based healthcare ecosystem. With the use of AI based camera monitoring, it could be used to monitor patients remotely, at their hospital beds without being tied down by a probe. Finally, with the direction of home-based remote healthcare monitoring, it could be used for remote, personalised monitoring at ones home, pertinent especially for the case of elderly population. NC TD-DOS has been used to demonstrate a proof-of-concept at small source-detector (ρ) and we will exploit a version of their setup and build on their work [2].

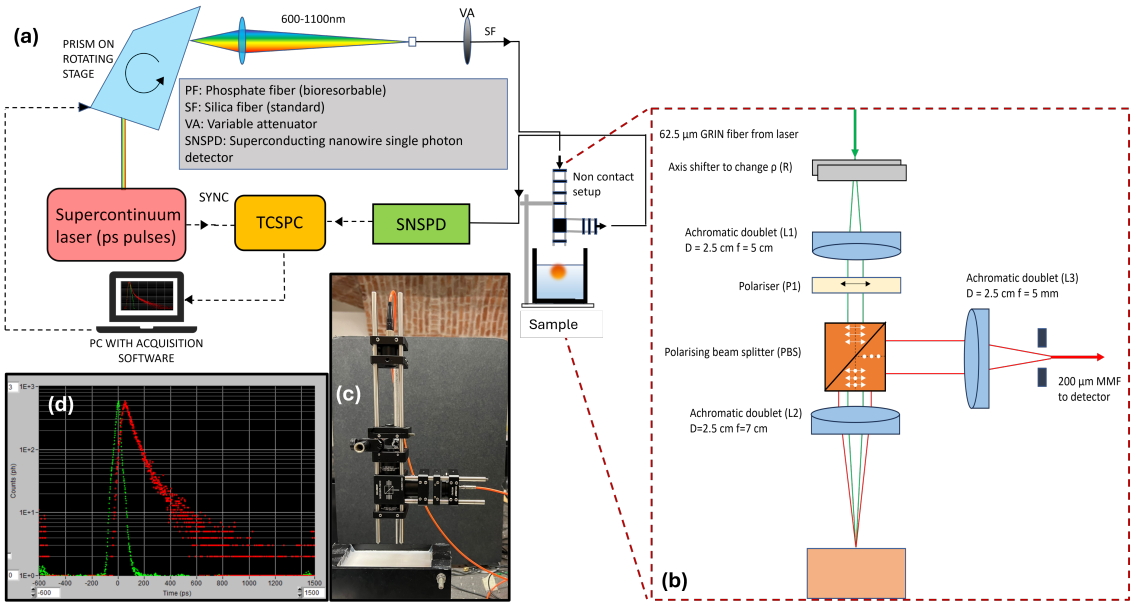

Fig. 1. (a) Schematic of the experimental setup, (b) Schematic of the non-contact probe, (c) Measurement on a liquid phantom, (d) DTOFs obtained from a measurement at 700 nm on a liquid phantom.

Diffuse Optical Spectroscopy and Imaging X, edited by Davide Contini, Yoko Hoshi, Thomas D. O'Sullivan, Proc. of SPIE-Optica Vol. 13935, 1393513 · 2025
Published by SPIE-Optica · 1605-7422 · doi: 10.1117/12.3098386

2. Materials and methodology

Measurements were acquired using a state-of-the-art TD-DOS system [3]. Picosecond pulses at 40 MHz from a supercontinuum laser (SuperK Extreme, NKT Photonics) were spatially dispersed using a Pellin-Broca prism, which was mounted on a precision rotating stage to permit wavelength selection by adjusting its rotation, thus enabling scanning from 600–1100 nm. The light was coupled into the sample through a 62 μm core fiber, through a variable attenuator to regulate the input power and into the NC probe. The probe design requires the use of optically optimized designs to deal with beam divergence and direct reflections. The probe employs a collinear geometry, as shown in Fig. 1(b), exploiting the previous work [2]. It utilizes polarized incident beams and optics to reject direct reflections and thus preserve the dynamic range of the detector. It is worth noting that rejection of direct reflection is not sufficient to suppress the burst of early photons at null source-detector separation [4] and hence a high dynamic range detector - a superconducting nanowire single photon detector (SNSPD; Single Quantum BV, Netherlands) is used to detect the photons collected by the NC probe. It converts detected photons into voltage pulses, which are processed by a time-correlated single-photon counting (TCSPC) board (SPC-130, Becker Hickl) to generate a timing histogram of photon arrival times, i.e. the DTOF curve. Fig. 1(d) shows the instrument response function (IRF) in green and a sample DTOF in red obtained for a liquid phantom at 700 nm. The important point to note is the clean IRF of the SNSPD which has an almost Gaussian response and lacks any tails or background noise thus allowing us to obtain upto 4 orders of dynamic range. For this first campaign of measuremenst, we used H=7 cm and a source-detector separation ρ=0.5 cm

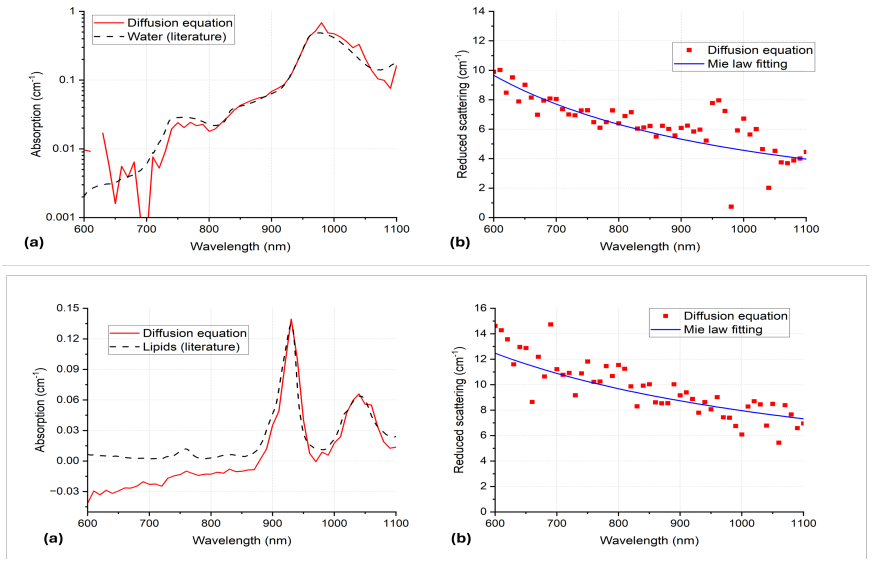

Fig. 2. μ_a and μ_s' spectra of the water+IL phantom - (a) and (b), and of the lipid phantom - (c),(d).

3. Phantom measurements

Initial measurements were performed on (i) a liquid phantom of water+intraipid, with a nominal scattering of 12 cm^{-}1 at 700 nm, and (ii) a solid lipid phantom of porcine fat. From Fig. 2(a), the retrieved absorption spectrum of the water + IL phantom resembles that of water from literature within a relative error of 20% in the range of 750 - 1060 nm. The discrepancies at lower wavelengths can be explained due to the low absolute value of absorption, while those at longer wavelengths arise due to higher background noise due to the presence of the pump laser at 1064 nm. The scattering in Fig. 2(b) on the other hand has a marginally lower value than the expected nominal value of 12 cm^{-1} at 700 nm. Figures 2(c) and (d) on the other hand show the same information for the fat phantom. The μ_s' seems within expected values and appears to the follow the Mie scattering law. While the well known lipid peaks at 920 and 1040 nm are resolved reasonably well, there is a large underestimation of the absorption below 900 nm, with the retrieval also of non-physical, negative values. In general, while the shape of the absorption spectra are resolved well, the absolute values are not always consistent with literature an this will be addressed later.

4. Preliminary in-vivo study

We then attempted a preliminary in-vivo protocol on 10 healthy subjects. Measurements were performed on the anterior forearm with the NC probe as well a standard contact probe for reference. Fig. 3 shows the μ_a and μ_s' for three best subjects - 2, 7 and 8. In general, all the μ_a spectra have three important features - (i) high absorption below 700 nm due to blood components in muscle, (ii) a conspicuous high absorption 'bump' around 980 nm due to presence of water, a prominent chromophore in the muscle, and (iii) a smaller yet, noticeable peak around 920 nm for most subjects, given that we are not probing too deep into the muscle tissue as compared to superficial adipose layers. While the two systems yield similar spectra, the discrepancies between the absolute values are noticeable too. As regards the μ_s' spectra in Fig. 3, the values retrieved are in the expected range for a human

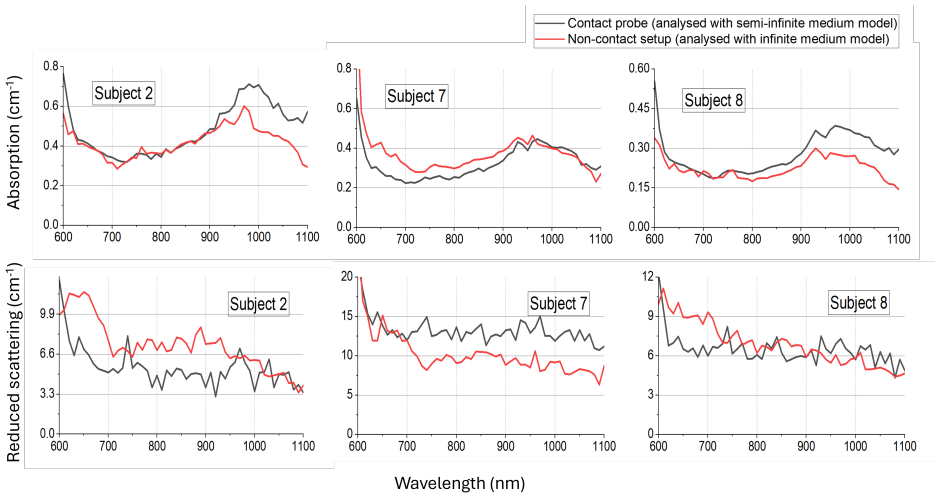

Fig. 3. *(Top row)* Absorption and *(bottom row)* reduced scattering spectra of three subjects.

forearm and the two probes are within reasonable difference of each other. Finally, the μ_a spectra for subjects 2, 7 and 8 bear the closest resemblance to each other and this is also reflected in the μ_s' spectra of these subjects having lesser differences. The discrepancies in the retrieval of optical properties could be due to various reasons. Firstly, existing inverse models lack accurate boundary conditions for NC measurements as regular Zero boundary conditions or Partial current boundary conditions cannot be applied here. Secondly, optical AR coatings cause increased reflections beyond 1000 nm. While the laser is stable, SNSPDs optimized for specific wavelengths (830 nmin this case) lose efficiency at longer wavelengths, leading to signal loss and noisy spectra. Finally, polarization-based rejection improves signal quality but reduces efficiency due lots of signal loss.

5. Conclusions

We were able perform broadband TD-DOS in a NC geometry at a distance of H=7 cm on both phantoms and human subjects using an SNSPD. We compared the results to either literature or a standard system and were able to get good preliminary results. However, there still exists a long road with need for better analysis strategies, IRF considerations, efficiency improvements, detection techniques, etc.

Acknowledgements

The authors acknowledge funding from (i) Horizon 2020 PHAST-ETN (ID: 860185); (ii) Next Generation EU I-PHOQS (R0000016, ID D2B8D520); (iii) Next Generation EU - "PNRR - M4C2, investment 1.1 - "PRIN 2022 fund" (ID 20225MR35K); (iv)

References

1. A Pifferi, "New frontiers in time-domain diffuse optics, a review," J. of biomed. opt.**21(9)**, 091310–091310 (2016).
2. Di Sieno, L, et al. "Characterization of a time-resolved non-contact scanning diffuse optical imaging system exploiting fast-gated single-photon avalanche diode detection." Rev. of Sci. Inst. 87.3 (2016).
3. Damagatla, V, et al. "Interstitial null-distance time-domain diffuse optical spectroscopy using a superconducting nanowire detector." J. Biomed. Opt. 28.12 (2023): 121202-121202.
4. Torricelli, A, et al. "Time-Resolved Reflectance at Null Source-Detector Separation" Phy. rev. lett. 95.7 (2005): 078101.